MATEC Web of Conferences **33**, 05002 (2015)
DOI: 10.1051/matecconf/20153305002

First Principles and Monte Carlo Calculations of Structural and Magnetic Properties of $Fe_xNi_{2-x}Mn_{1+y}Al_{1-y}$ Heusler Alloys

Mikhail Zagrebin[1,2,a], Vladimir Sokolovskiy[1,3], Marina Klyuchnikova[1] and Vasiliy Buchelnikov[1]

[1]*Chelyabinsk State University, Condensed Matter Physics Department,454001 Chelyabinsk, Russia*
[2]*National Research South Ural State University, Mathematical Physics Equations Department, 454080 Chelyabinsk, Russia*
[3]*National University of Science and Technology "MIS&S", Moscow, 119049, Russia*

Abstract. The composition dependences of crystal lattice parameters, bulk moduli, magnetic moments, magnetic exchange parameters, and Curie temperatures in $Fe_xNi_{2-x}Mn_{1+y}Al_{1-y}$ ($0.2 \le x \le 1.8$; $0.0 \le y \le 0.6$) Heusler alloys are investigated with the help of first principles and Monte Carlo calculations. It is shown that equilibrium lattice parameters and Mn_Y-Mn_Z magnetic exchange interactions increase with increasing Fe content (x). A crossover from ferromagnetic to antiferromagnetic interaction between nearest neighbors Mn_Y and Mn_Z atoms was observed in compositions with $x \ge 1.4$ and $0.2 \le y \le 0.6$. Such magnetic competitive behavior points to a complex magnetic structure in $Fe_xNi_{2-x}Mn_{1+y}Al_{1-y}$. Calculated values of lattice parameters, magnetic moments, and Curie temperatures are in a good agreement with other theoretical results and available experimental data.

1 Introduction

Nowadays, Heusler alloys have attracted a huge interest because of various effects (such as the shape memory, magnetocaloric effect (MCE), exchange bias, and superelasticity) and their potential applications as intelligent functional materials [1-3]. In recent years, novel $Fe_{2+x}Mn_{1-x}Al$ Heusler compounds have been intensively investigated by experimentalists and theoreticians [4-6]. These magnetic materials are considered to be very promising for technological applications utilizing their properties such as anomalous behaviours of optical, magnetic and transport properties.

One of the ways to enhance the magnetic and structural properties of Fe-Mn-Al system is related to addition of fourth 3*d* element. Recent experiments have shown that the substitution of 7.5% of Fe for Ni in the $Fe_{51}Mn_{34}Al_{15}$ results in an enhancement of the super-elastic behavior observed over a wide temperature range from 77 to 513 K [9-11]. A good room-temperature strength and a significant ductility was found in the $Fe_{30}Ni_{20}Mn_{35}Al_{15}$ alloy with a higher Ni content [7, 8]. Further increase in Ni content leads to increase in MCE. Thus, the positive magnetic entropy change ($\Delta S \approx 3.35$ J/kgK) in $Ni_{44}Fe_6Mn_{32}Al_{18}$ under magnetic field change of 30 kOe has been found by Xuan et al. [12]. Based upon the information, we can suggest that the families of $Fe_xNi_{2-x}Mn_{1+y}Al_{1-y}$ compositions are the promising candidates in the development of multifunctional materials.

In this work, we present the *ab initio* and Monte-Carlo calculations of structural and magnetic properties of series of $Fe_xNi_{2-x}Mn_{1+y}Al_{1-y}$ ($0.2 \le x \le 1.8$, $0.0 \le y \le 0.6$) compounds.

2 Calculation details

2.1 *Ab initio* calculation details

All the calculations were performed using the density functional theory as part of the spin-polarized relativistic Korringa-Kohn-Rostoker (SPR-KKR) package [13, 14]. This code is based on the KKR-Green's function formalism that makes possible using of the multiple-scattering theory, and the electronic structure is expressed in terms of the corresponding Green's function as opposed to Bloch wave functions and eigenvalues. In this code, a chemical disorder is treated through the coherent potential approximation [14]. The generalized gradient approximation for the exchange correlation functional in the formulation of Perdew, Burke and Ernzerhof was taken into account [16]. The SPR-KKR was used to determine the equilibrium parameter of a cubic $L2_1$ structure with ferromagnetic (FM) order. Where, all magnetic moments of Fe, Ni and Mn atoms are parallel [5]. It should be pointed out that the $L2_1$ cubic structure can be represented as four interpenetrating *fcc* sublattices with Al at site (0, 0, 0), Mn at site (1/2, 1/2, 1/2) and two Fe at sites (1/4, 1/4, 1/4) and (3/4, 3/4, 3/4), respectively. In order to formation of off-stoichiometric Fe-Ni-Mn-Al alloys, the excess of Ni and Mn were randomly located at Fe and Al sites. Therefore, we use follow designations: Mn_Y and Mn_Z. Where, Mn_Y atoms are located at regular Mn sublattice and Mn_Z atoms are

[a] Corresponding author: miczag@mail.ru

Article available at http://www.matec-conferences.org or http://dx.doi.org/10.1051/matecconf/20153305002

occupied the Al sublattice. For the optimized lattice parameter the magnetic exchange coupling parameters J_{ij} were calculated by using the expression proposed by Liechtenstein et al. [15], which is employed in the SPR-KKR package.

2.2 Monte Carlo Hamiltonian

In order to simulate temperature dependences of the qualitative dependence of the Curie temperature in the austenite, we used the q-state Potts Hamiltonian with different q states for the magnetic atoms. As it is well known, the Potts model allows to describe both first and second order phase transitions observed in Heusler alloys in comparison with the Heisenberg model. We would like to mention that critical temperatures obtained by the Potts model are consistent with the results obtained by Heisenberg model. A reader can find the addition information about it in Ref. [17]. Since our goal is related to estimation of the Curie temperature of austenite that we will take into account only a magnetic part of the total Hamitonian with "*ab initio*" exchange coupling constants.

We note that the information about total Hamiltonian containing magnetic, elastic, and magnetoelastic terms is presented in Ref. [18]. Therefore, the magnetic part of Hamiltonian at zero magnetic field can be written as:

$$H = -\sum J_{ij}\delta_{s_i,s_j}, \qquad (1)$$

where J_{ij} are exchange coupling constants between magnetic atoms at sites i and j, which are taken from *ab initio* calculations. S_i is the magnetic degree of freedom at site i which can take on q integer values depending on the total spin moment S of an atom. The Kronecker symbol δ_{s_i,s_j} restricts the spin-spin interactions to the interactions between the same S_i states for Fe, Ni and Mn. Three-dimensional lattice containing 3925 atoms with periodic boundary conditions was considered. The simulations were carried out by using using the classical Metropolis algorithm [18].

3 Computational Results

3.1 Equilibrium lattice parameter and bulk modulus

The equilibrium lattice parameter in austenite of $Fe_xNi_{2-x}Mn_{1+y}Al_{1-y}$ as a function of Fe excess (x) at different values of Mn excess (y) is presented in Fig. 1. It is seen that lattice constants decrease with increasing Fe content. It should be noted that our theoretical lattice parameters for Ni_2MnAl and Fe_2MnAl are in a good agreement with results obtained from another *ab initio* calculations [5, 19]. Obtained equilibrium lattice parameters were used for subsequent calculations of magnetic properties of $Fe_xNi_{2-x}Mn_{1+y}Al_{1-y}$ alloys.

In Figure 2 we present the contour plot of a bulk modulus for $Fe_xNi_{2-x}Mn_{1+y}Al_{1-y}$ projected on the plane (x, y). As can be seen the bulk modulus decreases until $x \approx 1.25$ and further decreases with increasing Fe excess. The smallest value of a bulk modulus (≈ 85 GPa) is found for the $Fe_{0.2}Ni_{1.8}Mn_{1.6}Al_{0.4}$ composition.

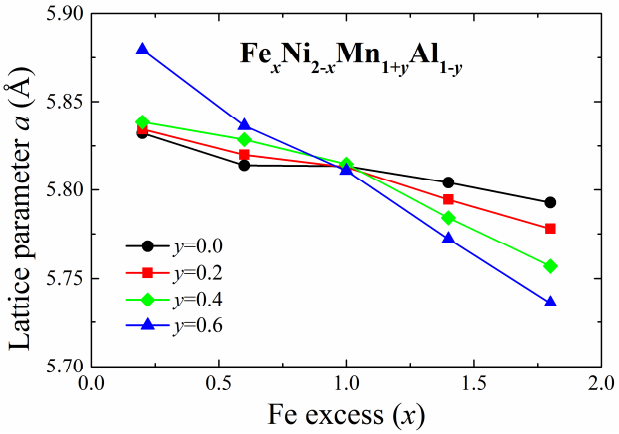

Figure 1. Equilibrium lattice parameter in austenite of $Fe_xNi_{2-x}Mn_{1+y}Al_{1-y}$ for different value of Mn excess (y) as a function of Fe excess (x).

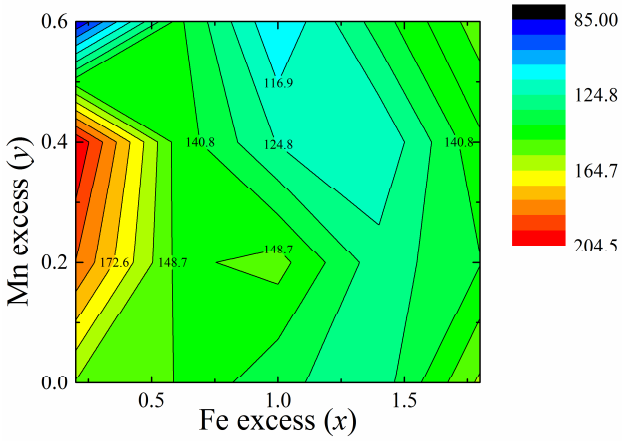

Figure 2. The bulk modulus contour in austenite of $Fe_xNi_{2-x}Mn_{1+y}Al_{1-y}$ for different value of Fe (x) and Mn excesses (y).

3.2 Spin magnetic moment

In this subsection we discuss calculation results of partial and total magnetic moments of $Fe_xNi_{2-x}Mn_{1+y}Al_{1-y}$ alloys. In Fig. 3a we depict the distribution of a total magnetic moment mapped on the plane (x, y). The same distribution of Fe moment shown in Fig. 3b. It can be seen from Figure 3a that the total magnetic moment increases with increasing Mn content. The lowest (highest) value of a magnetic moment is closed to 4 (7) μ_B for $Fe_{0.2}Ni_{1.8}MnAl$ ($Fe_{1.0}Ni_{1.0}Mn_{1.6}Al_{0.4}$) composition, respectively. The dependences of partial magnetic moment of Fe atoms have a complex behavior (Fig. 3b).

3.3 Magnetic exchange constants

Figure 4 displays the magnetic exchange parameters in austenitic phase of $Fe_{0.2}Ni_{1.8}Mn_{1.2}Al_{0.8}$ (Fig. 4a) and $Fe_{1.8}Ni_{0.2}Mn_{1.4}Al_{0.6}$ (Fig. 4b) as functions of a distance between pairs of atoms. These compositions are closed to experimental compositions $Ni_{44}Fe_6Mn_{32}Al_{18}$ and

$Fe_{43.5}Ni_{7.5}Mn_{34}Al_{15}$ showing the promising magnetocaloric and superelastic properties [9-11]. Here and further, the positive exchange constants ($J_{ij} > 0$) are characterized the FM coupling, whereas the negative ones ($J_{ij} < 0$) point to the antiferromagnetic (AF) coupling. The oscillating damped behavior of J_{ij} can be observed from Figure 4. We would like to note that this trend is typical for the RKKY-exchange interaction [20]. In the case of $Fe_{0.2}Ni_{1.8}Mn_{1.2}Al_{0.8}$, the strongest FM interaction between nearest-neighbor (NN) Fe-Mn_Y and Ni-$Mn_{Y,Z}$ atoms can be seen from Fig. 4a. Note, that values of these interactions are approximately closed to 7 meV. The AF interaction is observed between NN Mn_Y-Mn_Z atoms in the first coordination sphere. The Fe-Fe interaction is the FM one and it is closed to zero. In regard to the second coordination shell, we can see that this interaction is also closed to zero, but its nature is AF. Contrary to that the Fe-Fe interaction within the third coordination sphere splits into two interactions: weak FM and strong AF (≈ -5 meV) ones. On the other hand, the fourth NN interaction between Fe atoms becomes the FM one. This clearly demonstrates the competitive behavior between the FM and AF interactions. The Fe-Mn_Z interaction is FM and it equals 2 meV.

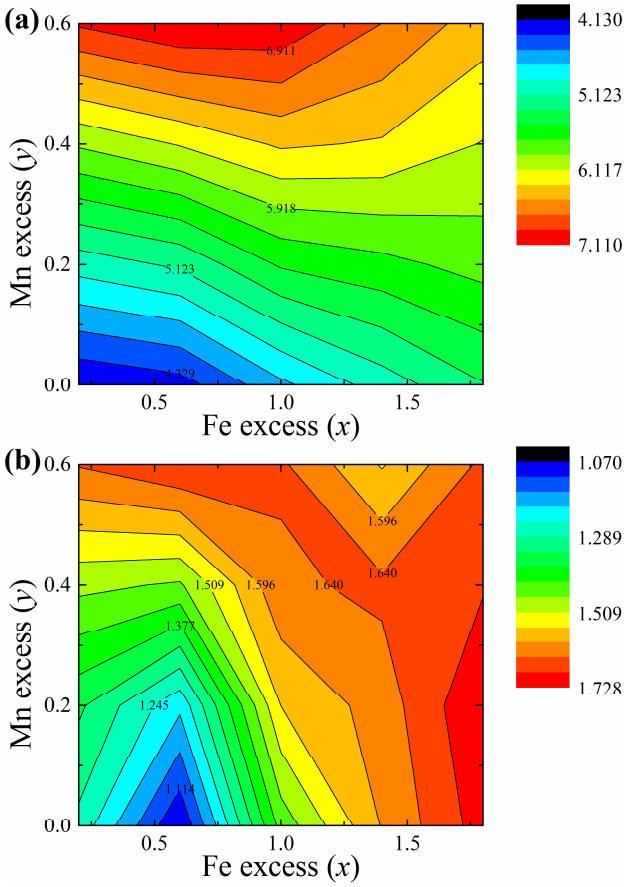

Figure 3. The magnetization contour in austenite of $Fe_xNi_{2-x}Mn_{1+y}Al_{1-y}$ for different value of Fe (x) and Mn excesses (y). a) total magnetization; b) partial magnetization of Fe atoms.

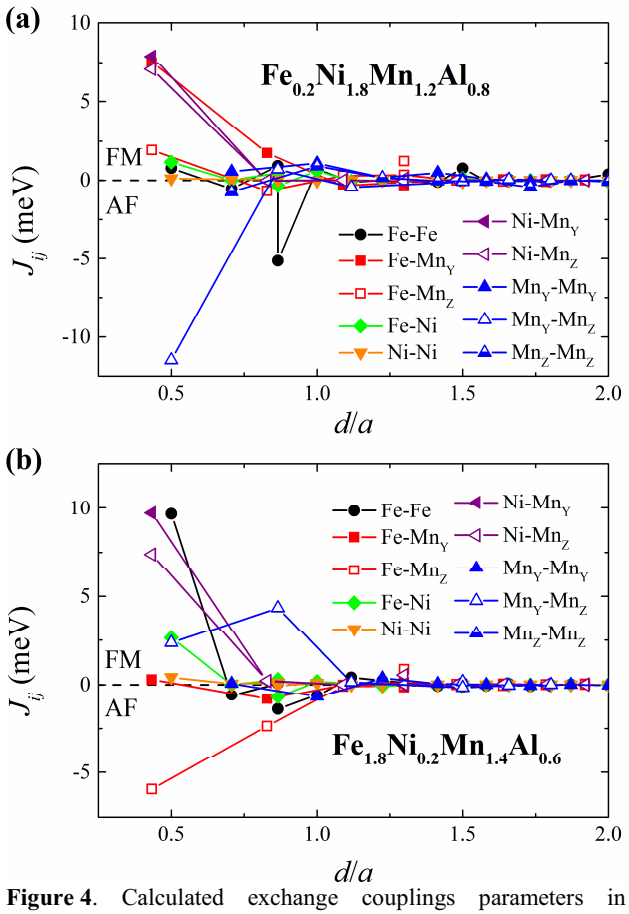

Figure 4. Calculated exchange couplings parameters in austenite of $Fe_xNi_{2-x}Mn_{1+y}Al_{1-y}$ as a function of a distance between pairs of atoms i and j (in units of the lattice constant a). a) $Fe_{0.2}Ni_{1.8}Mn_{1.2}Al_{0.8}$; b) $Fe_{1.8}Ni_{0.2}Mn_{1.4}Al_{0.6}$.

Let us discuss the exchange interactions for the $Fe_{1.8}Ni_{0.2}Mn_{1.4}Al_{0.6}$ composition. We can see that Fe-Fe and Fe-Ni interactions increase, while Fe-$Mn_{Y,Z}$ interactions are found to decrease at the crossover from $Fe_{0.2}Ni_{1.8}Mn_{1.2}Al_{0.8}$ to $Fe_{1.8}Ni_{0.2}Mn_{1.4}Al_{0.6}$ alloy. Besides, the Fe-Mn_Y exchange goes to zero while the Fe-Mn_Z (Mn_Y-Mn_Z) ones change their sign from positive (negative) to negative (positive), respectively. A strong competitive behavior between FM and AF interactions clearly shows that these alloys have a complex magnetic structure.

The behaviors of exchange coupling parameters between nearest Mn_Y-Mn_Z and Fe-Fe atoms in austenite of $Fe_xNi_{2-x}Mn_{1+y}Al_{1-y}$ as a function of Fe content (x) are depicted in Figure 5. We can see from Fig. 5a that the Fe-Fe interaction shows a non-linear behavior characterizing by an increase and a decrease in Fe=Fe coupling for all compositions with $0.0 \le y \le 0.6$. The largest FM interaction (about 27 meV) is observed between Fe atoms for composition with $x = 0.6$ and $y = 0.6$. With respect to the Mn_Y-Mn_Z interaction shown in Fig. 5b, it is seen that the substitution of Fe for Ni leads to a linear increase in this interaction. Moreover, the crossover between AF/FM exchange interactions can be observed at compositions with $x = 1.5$ and $y \le 0.4$. Obtained values of magnetic exchange constants were used for further simulations of magnetization curves for $Fe_xNi_{2-x}Mn_{1+y}Al_{1-y}$ alloys as functions of a temperature by the Monte Carlo method.

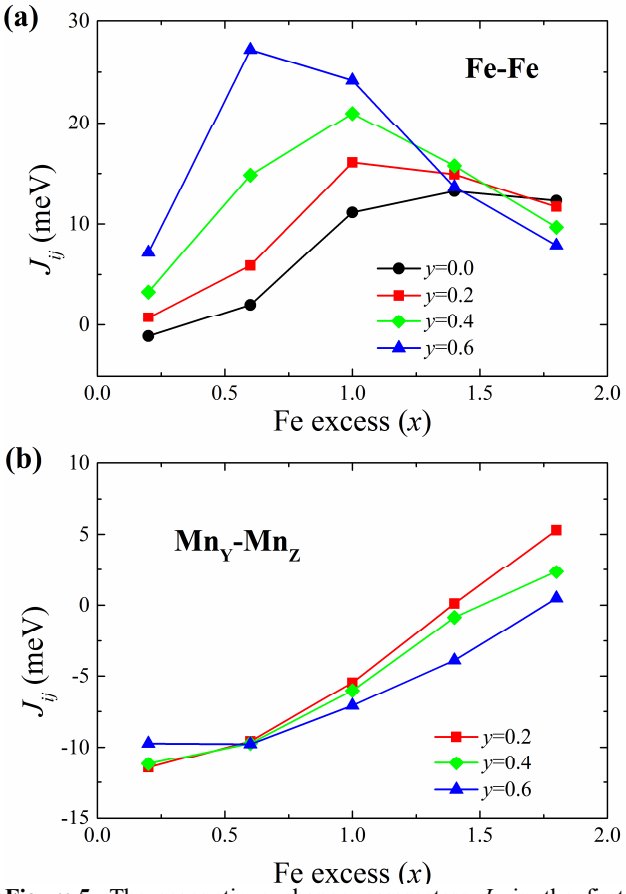

Figure 5. The magnetic exchange parameters J_{ij} in the first coordination sphere in austenite of $Fe_xNi_{2-x}Mn_{1+y}Al_{1-y}$ as a function of Fe excess (x). a) Fe-Fe coupling; b) Mn_Y-Mn_Z coupling.

3.4 Curie temperature

The temperature dependences of magnetizations in austenitic phase of $Fe_{0.2}Ni_{1.8}Mn_{1.2}Al_{0.8}$ and $Fe_{1.8}Ni_{0.2}Mn_{1.4}Al_{0.6}$ under zero magnetic field are shown in Figure 6.

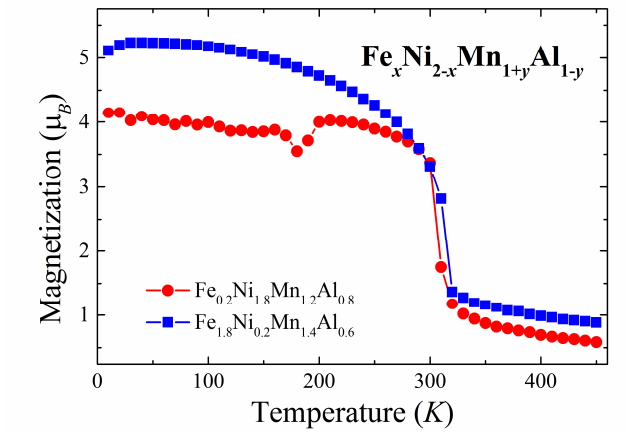

Figure 6. Magnetization M in austenite of $Fe_xNi_{2-x}Mn_{1+y}Al_{1-y}$ as a function of temperature T.

We can see that the Curie temperatures of austenite are 307 and 316 K for $Fe_{0.2}Ni_{1.8}Mn_{1.2}Al_{0.8}$ and $Fe_{1.8}Ni_{0.2}Mn_{1.4}Al_{0.6}$ alloys, respectively. These values are in a good agreement with experimental data for $Ni_{44}Fe_6Mn_{32}Al_{18}$ and $Fe_{43.5}Ni_{7.5}Mn_{34}Al_{15}$ alloys [9-11].

In Fig. 7 we show calculation results of theoretical Curie temperature of austenite for $Fe_xNi_{2-x}Mn_{1+y}Al_{1-y}$ ($0.2 \le x \le 1.8$; $0.0 \le y \le 0.6$) compositions as a function of Fe content. These data were taken from thermomagnetization curves simulated by Monte Carlo technique. Our calculations have shown that for compositions containing the Mn excess ($y > 0$) the Curie temperatures firstly increase and further decrease with increasing Fe excess (x). But for compositions with $y = 0$ it is found to decrease with increase of x content. The largest value of T_C (≈ 455 K) is observed for composition with $x = 1.4$ and $y = 0.6$.

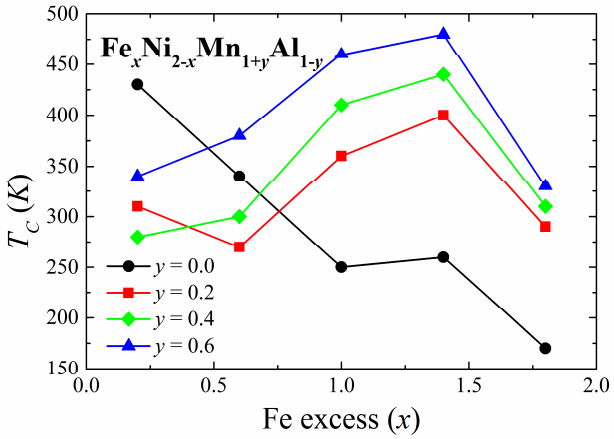

Figure 7. Calculated Curie temperature in austenite of $Fe_xNi_{2-x}Mn_{1+y}Al_{1-y}$ for different value of Mn excess (y) as a function of Fe excess (x).

The main obtained results are listed in Table 1.

4 Summary

The composition dependence of crystal lattice parameters, bulk moduli, magnetic moments, magnetic exchange parameters, and Curie temperatures of austenite in $Fe_xNi_{2-x}Mn_{1+y}Al_{1-y}$ ($0.2 \le x \le 1.8$; $0.0 \le y \le 0.6$) Heusler alloys have been calculated using a combination of first principles and Monte Carlo approaches. The equilibrium lattice parameters were found to increase with increasing Fe content (x). The strong competitive behavior between FM and AF interactions is the reason of a complex magnetic structure. An increase of Fe content results in an increase of exchange magnetic interactions between Mn atoms at regular positions and Mn atoms located at Al positions. The crossover from AF to FM interaction was found for compositions with $y = 1.4$. Calculated values of lattice parameters and magnetic moments are in a good agreement with theoretical and experimental data [21]. It should be noted that for more complete understanding of crystal and magnetic structure it is necessary to investigate different magnetic structures.

Table 1. Calculated equilibrium lattice constant a, bulk modulus B, spin magnetic moment m and Curie temperature of austenite T_C^A, of $Fe_xNi_{2-x}Mn_{1+y}Al_{1-y}$ alloys.

Composition	a, Å	B, GPa	m, μB	T_C^A, K
$Fe_{0.2}Ni_{1.8}Mn_{1.0}Al_{1.0}$	5.83	155.8	4.13	430
$Fe_{0.6}Ni_{1.4}Mn_{1.0}Al_{1.0}$	5.81	148.5	4.23	340
$Fe_{1.0}Ni_{1.0}Mn_{1.0}Al_{1.0}$	5.81	134.5	4.68	250
$Fe_{1.4}Ni_{0.6}Mn_{1.0}Al_{1.0}$	5.80	128.2	5.02	260
$Fe_{1.8}Ni_{0.2}Mn_{1.0}Al_{1.0}$	5.79	158.4	5.31	170
$Fe_{0.2}Ni_{1.8}Mn_{1.2}Al_{0.8}$	5.83	188.3	5.01	310
$Fe_{0.6}Ni_{1.4}Mn_{1.2}Al_{0.8}$	5.82	146.8	5.16	270
$Fe_{1.0}Ni_{1.0}Mn_{1.2}Al_{0.8}$	5.81	151.8	5.55	360
$Fe_{1.4}Ni_{0.6}Mn_{1.2}Al_{0.8}$	5.79	128.3	5.66	400
$Fe_{1.8}Ni_{0.2}Mn_{1.2}Al_{0.8}$	5.79	140.3	5.79	290
$Fe_{0.2}Ni_{1.8}Mn_{1.4}Al_{0.6}$	5.84	204.1	5.95	280
$Fe_{0.6}Ni_{1.4}Mn_{1.4}Al_{0.6}$	5.83	145.6	6.13	300
$Fe_{1.0}Ni_{1.0}Mn_{1.4}Al_{0.6}$	5.82	124.3	6.35	410
$Fe_{1.4}Ni_{0.6}Mn_{1.4}Al_{0.6}$	5.78	117.3	6.29	440
$Fe_{1.8}Ni_{0.2}Mn_{1.4}Al_{0.6}$	5.78	147.1	6.11	310
$Fe_{0.2}Ni_{1.8}Mn_{1.6}Al_{0.4}$	5.88	85.2	6.94	340
$Fe_{0.6}Ni_{1.4}Mn_{1.6}Al_{0.4}$	5.84	143.1	7.11	380
$Fe_{1.0}Ni_{1.0}Mn_{1.6}Al_{0.4}$	5.81	109.1	7.07	460
$Fe_{1.4}Ni_{0.6}Mn_{1.6}Al_{0.4}$	5.77	137.0	6.71	480
$Fe_{1.8}Ni_{0.2}Mn_{1.6}Al_{0.4}$	5.74	161.5	6.41	330

Acknowledgments

This work was supported by Russian Science Fund No. 14-12-00570 (Section 1), Ministry of Education and Science RF No. 3.2021.2014/K (Section 4), RFBR (grants 14-02-01085, 14-02-31189).

References

1. V.D. Buchel'nikov, A.N. Vasiliev, V.V. Koledov, S.V. Taskaev, V.V. Khovailo, and V.G. Shavrov. Phys. Usp. **49**, 871 (2006).
2. P. Entel, M.E. Gruner, A. Dannenberg, M. Siewert, S.K. Nayak, H.C. Herper, and V. Buchelnikov. Mater. Sci. Forum **635**, 3 (2010).
3. G.A. Perez Alcazar, L.E. Zamora, and A. Bohorquez. J. Appl. Phys. **79**, 6155 (1996).
4. S.M. Azar, B.A. Hamad, and J.M. Khalifeh. J. Magn. Magn. Mater. **324**, 1776 (2012).
5. V.D. Buchelnikov, M.A. Zagrebin, V.V. Sokolovskiy, I.A. Taranenko, and A. T. Zayak. Phys. Status Solidi C **11**, 979 (2014).
6. R. Umino, X.J. Liu, Y. Sutou, C.P. Wang, I. Ohnuma, R. Kainuma, and K. Ishida. J. Phase Equilib. Diff. **27**, 54 (2006).
7. Y. Liao and I. Baker. Mater. Charact. **59**, 1546 (2008).
8. I. Baker, X. Wu, F. Meng, and P.R. Munroe. Mater. Sci. Forum **783**, 786 (2014).
9. T. Omori, K. Ando, M. Okano, X. Xu, Y. Tanaka, I. Ohnuma, R. Kainuma, and K. Ishida. Science, **333**, 68 (2011).
10. T. Omori, M. Okano, and R. Kainuma. APL Materials **1**, 032103 (2013).
11. L.W. Tseng, Ji. Ma, S.J.Wang, I. Karaman, M. Kaya, Z.P. Luod, and Y.I. Chumlyakov. Acta Mater. **89**, 374 (2015).
12. H.C. Xuan, Y.Q. Zhang, H. Li, P.D. Han, D.H. Wang, and Y. W. Du. Appl. Phys. A.-Mater. **119**, 597 (2015).
13. H. Ebert. SPRKKR package (version 6.3). http://ebert.cup.uni-muenchen.de/.
14. .H. Ebert, D. Kodderitzsch, and J. Minar. Rep. Prog. Phys., **74**, 096501 (2011).
15. A.I. Liechtenstein, M.I. Katsnelson, V.P. Antropov, and V.A. Gubanov. J. Magn. Magn. Mater. **67**, 65 (1987).
16. J.P. Perdew, K. Burke, and M. Ernzerhof. Phys. Rev. B. **77**, 3865 (1997).
17. V.V. Sokolovskiy, O. Pavlukhina, V.D. Buchelnikov and P. Entel. J. Phys. D: Appl. Phys. **47**, 425002 (2014).
18. V.D. Buchelnikov, V.V. Sokolovskiy, H.C. Herper, H. Ebert, M.E. Gruner, S.V. Taskaev, V.V. Khovaylo, A. Hucht, A. Dannenberg, M. Ogura, H. Akai, M. Acet, and P. Entel. Phys. Rev. B, **81**, 094411 (2010).
19. T. Busgen, J. Feydt, R. Hassdorf, S. Thienhaus, M. Moske, M. Boese, A. Zayak, and P. Entel. Phys. Rev. B, **70**, 014111 (2004).
20. C. Kittel. Introduction to Solid State Physics (Wiley & Sons Inc, 2005).
21. V.D. Buchelnikov, M.A. Klyuchnikova, M.A. Zagrebin, and V.V. Sokolovskiy. Sol. State Phenom. **233-234**, 187 (2015).